RSC Advances

PAPER

View Article Online
View Journal | View Issue

Cite this: *RSC Adv.*, 2015, **5**, 42603

Shape-controlled synthesis and lithium storage properties of SnO_2 nonspherical hollow structures†

Yong Wang,* Panshuang Ding and Xiaowen Su

Received 4th May 2015
Accepted 7th May 2015

DOI: 10.1039/c5ra08232c

www.rsc.org/advances

In this work, a variety of uniform SnO_2 nonspherical hollow structures, such as peanuts, capsules and pseudocubes, can be synthesized by using monodisperse hollow silica nonspherical colloids with different shapes as templates. The method is based on a polycrystalline SnO_2 coating on the surface of the hollow silica colloidal template with different shapes and the sequential HF-dissolution of the silica. It is noted that the shapes of these SnO_2 nonspherical hollow structures are similar to those of the colloidal templates. By virtue of the hollow interior voids, the SnO_2 hollow structures with different shapes exhibit improved lithium storage properties compared to SnO_2 solid spheres.

Introduction

Hollow micro-/nanostructures with controlled shape, size, shell composition, and internal structure have attracted great interest owing to their potential applications in lithium batteries, gas sensors, solar cells, photocatalysis, catalysis, bimolecular-release systems, and so on.[1–6] To satisfy the different requirements of such applications, hollow materials with varying sizes and shapes have been synthesized by a number of methods, such as an electrospinning technique,[7] hydrothermal methods,[8,9] biomolecule-assisted routes,[10] and soft- and hard-templating methods.[11–13] Templated synthesis is a straightforward method for the shape control of materials, because the resultant shapes originating from the sacrificed templates are quite predictable.[14] Recently, some nonspherical templates, such as $MnCO_3$ cubes,[15,16] Cu_2O cubes,[17] and Fe_2O_3 nanospindles,[18] have been used to synthesize metal oxides with nonspherical hollow structures. Notwithstanding these advances, the shapes of the nonspherical hollow products are still difficult to control by conventional templating methods, because suitable templates with different shapes for the nonspherical hollow products are often not available.[19] Thus, it remains a great challenge to develop new templating routes based on nonspherical templates with well-dispersion and diverse shapes for the shape-controlled synthesis of nonspherical hollow metal oxides.

Tin dioxide is one of the most intensively studied materials owing to its technologically important applications such as gas sensors,[20] dye-sensitized solar cells (DSSCs),[21] supercapacitors,[22] and anode materials in lithium rechargeable batteries.[18,23] Recent researches on SnO_2 hollow spheres have indicated that hollow structures can improve the electrochemical properties of anode materials for lithium batteries.[24] More recently, silica-coated Fe_2O_3 spindles have been used as a sacrificial template to fabricate hollow SnO_2 nanococoons with movable Fe_2O_3 cores *via* a facile solution-phase route.[25] In this approach, however, the employed ellipsoidal Fe_2O_3/SiO_2 templates show limited morphologies. It is noteworthy that only cocoon-shaped SnO_2 hollow structures can be prepared by using ellipsoidal templates in this method, and it is still difficult to obtain SnO_2 hollow structures with other shapes, such as peanut- and pseudocube-shape. Therefore, it is still a big challenge to explore the use of monodisperse silica particles with other different shapes as sacrificial templates for the shape-controlled synthesis of SnO_2 hollow structures. Moreover, to meet the ever-increasing technological demand, it is necessary to discuss the structure–property relationship of SnO_2 hollow structures with different shapes for both fundamental study and practical application.

In our previous paper, TiO_2 hollow structures with different shapes have been fabricated by using α-Fe_2O_3 with different shapes as templates.[26] Recently, our group has reported a shape-controlled synthesis of various hollow silica colloids using hematite colloidal particles with different shapes as templates.[27] In this work, the as-prepared hollow silica colloids with different shapes, such as peanuts, capsules and pseudocubes, are used as effective sacrificial templates to synthesize SnO_2 hollow structures with different nonspherical shapes. As schematically illustrated in Fig. 1, polycrystalline SnO_2 is uniformly deposited onto silica hollow colloids with different nonspherical shapes to form double-shelled silica@SnO_2

Department of Chemistry, Capital Normal University, Beijing, 100048, China. E-mail: yongwang@home.ipe.ac.cn

† Electronic supplementary information (ESI) available: FESEM and TEM images of monodisperse SiO_2 hollow colloids with different shapes; EDX spectra and TEM images of double-shelled SiO_2@SnO_2 hollow structures with different shapes; EDX spectra and TEM images of SnO_2 hollow structures with different shapes; TEM, SAED and HRTEM images of SnO_2 solid spheres and SnO_2 hollow structures with different shapes; Coulombic efficiency of SnO_2 solid spheres and SnO_2 hollow structures with different shapes; SEM images of SnO_2 hollow structures with different shapes after 60 cycles. See DOI: 10.1039/c5ra08232c

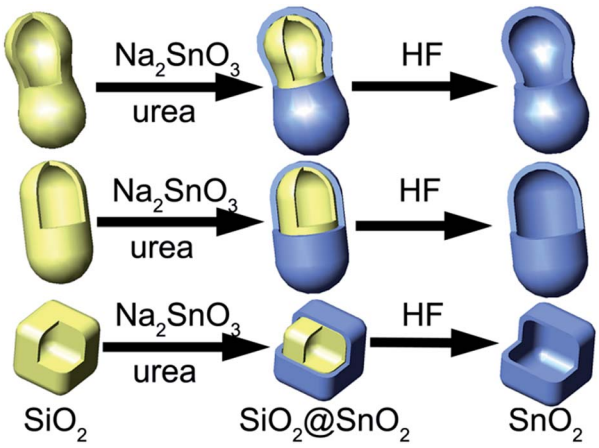

Fig. 1 Schematic procedure used for fabrication of SnO_2 nonspherical hollow structures with different shapes.

hollow structures, and then the silica is etched by HF solution, which results in the formation of the SnO_2 hollow structures with different nonspherical shapes. It is noted that the shapes of these SnO_2 hollow structures are similar to those of hollow silica templates. In addition, the electrochemical properties of the obtained hollow SnO_2 structures with different nonspherical shapes have also been investigated. To the best of our knowledge, this is the first report on the synthesis of peanut-shaped SnO_2 hollow structures as well as lithium storage capability of SnO_2 nonspherical hollow structures with different shapes.

Experimental

Preparation of silica hollow colloids with different shapes

All the reagents were of analytical grade, and used without further purification. Silica hollow colloids with different shapes were prepared as described in our previous study.[27] The synthesis of hollow silica colloids with different shapes, including hollow peanuts, hollow capsules and hollow pseudocubes, was achieved by a solution process using the prefabricated hematite colloidal particles with different shapes as sacrificial templates. The synthesis of hematite colloidal particles with different shapes was achieved by a process based on a method developed by Sugimoto *et al.*[28] For a typical silica coating, hematite colloidal particles (0.6 g) with different shapes were first dispersed by ultrasonication in a mixture consisting of 100 mL of ethanol and 5 mL of deionized water, followed by the addition of 15 mL of $NH_3 \cdot H_2O$ (28%). The mixture was poured into a 250 mL Pyrex bottle, which was then placed in an ultrasonic water bath under 50 °C. Then, 0.3 mL of Tetraethyl orthosilicate (TEOS) was added. After aged for 5 h, the products were collected by filtration, washed three times with deionized water and ethanol before vacuum-drying at 80 °C for 10 h. The as-prepared hematite/silica core/shell particles were almost etched with HCl solution (4 M) at 100 °C for 48 h to obtain hollow silica colloids without hematite cores.

Preparation of SnO_2 hollow structures with different shapes

For the synthesis of SnO_2 hollow structures with different shapes, such as peanuts, capsules and pseudocubes, the procedure was similar except that the shapes of hollow silica colloids using as templates were different. Hollow silica colloids (1.0 g) were dispersed by ultrasonication in a mixture consisting 180 mL of ethanol, 18 mL of deionized water and 17 mL of ammonia (28%), and aged for 12 h. After the products were collected by filtration, SiO_2 particles (0.12 g) were dispersed in 28 mL of ethanol–water mixed solvent (9 mL ethanol and 19 mL water). To this suspension, urea (0.90 g) and potassium stannate trihydrate (0.123 g, $Na_2SnO_3 \cdot 3H_2O$) were added. After shaken by hand for about 5 min until the salts dissolved, the suspension was transferred to a 50 mL Teflon-lined stainless-steel autoclave, which was then heated in an air flow electric oven at 170 °C for 36 h. After the autoclave cooled down naturally, the particles were washed three times with deionized water and ethanol before vacuum-drying at 80 °C for 10 h. After annealing the particles at 600 °C for 8 h, the silica was dissolved in 0.6 wt% HF solution. At last, he products were collected by filtration, washed three times with deionized water and ethanol before vacuum-drying at 80 °C for 10 h.

Characterization

X-ray diffraction (XRD) patterns of the samples were recorded with X-ray powder diffraction (XRD, Bruker, D8 ADVANCE). The morphology and structure of the samples were further investigated by field emission scanning electron microscopy (FESEM, Hitachi, S-4800) with energy-dispersive X-ray (EDX) spectroscopy, and transmission electron microscopy (TEM, FEI Tecnai F20, 200 kV). The Brunauer–Emmett–Teller (BET) specific surface areas and pore size distributions of the resultant products were measured with a Quantachrome NOVA 1000e analyzer.

Electrochemical tests

Electrochemical experiments were performed using 2032-type coin cells assembled in an argon-filled glove box. The working electrodes were prepared by coating the slurry of the active material powders (70 wt%), acetylene black (15 wt%) and poly (vinylidene fluoride) (PVDF) (15 wt%) dissolved in *n*-methyl pyrrolidinone onto a Cu foil substrate. After drying under vacuum, the electrodes were cut to a 1×1 cm^2 size. Lithium foil was used as the counter electrode. The electrolyte was composed of $LiPF_6$ (1 M) dissolved in ethylene carbonate/dimethyl carbonate/ethylene methyl carbonate (EC/DMC/EMC) with the volume ratio of 1 : 1 : 1. The cells were charged and discharged on a LAND CT2001A system in the range of 0.005–2.5 V (*vs.* Li/Li^+) at a current density of 100 mA g^{-1}.

Results and discussion

The silica templates with different nonspherical shapes, such as peanuts, capsules and pseudocubes, were prepared as described in our previous study.[27] Fig. S1† shows FESEM and TEM images of the products, indicating that the silica hollow

colloids with different nonspherical shapes are well dispersed and nearly uniform with sizes in the range of 1–2 μm.

The gradual deposition of SnO_2 nanocrystallites on the outer surfaces of SiO_2 hollow colloids with different shapes led to the formation of double-shelled silica@SnO_2 hollow structures with different shapes (insets of Fig. S2†). The reaction mechanism had been reported in the ref. 23 In the current hydrothermal synthesis at 170 °C, urea reacted with H_2O to form NH_3 and CO_2 (eqn (1)). Because of the affinity of SnO_2 to the –OH groups surrounding the surfaces of the silica colloids with different shapes, the released CO_2 would react with H_2O to provide H^+ for the deposition of SnO_2 on the surface of silica colloids with different shapes (eqn (2)) while the released NH_3 could provide a basic medium for the dissolution of silica (eqn (3) and (4)). The element composition was further confirmed with energy dispersive X-ray (EDX) spectroscopy analysis under TEM. EDX spectra show strong Sn, Si and O signals (Fig. S2†).

$$CO(NH_2)_2 + H_2O \rightarrow CO_2 + 2NH_3 \quad (1)$$

$$CO_2 + SnO_3^{2-} \rightarrow SnO_2 + CO_3^{2-} \quad (2)$$

$$NH_3 + H_2O \leftrightarrow NH_4^+ + OH^- \quad (3)$$

$$SiO_2 + 2OH^- \rightarrow SiO_3^{2-} + H_2O \quad (4)$$

In order to further confirm the formation of double-shelled silica@SnO_2 hollow structures with different shapes, we investigated the selective removal of silica in HF solution. After the as-prepared double-shelled silica@SnO_2 hollow structures with different shapes were almost etched with HF solution, various SnO_2 hollow structures with different shapes, such as peanuts, capsules and pseudocubes, were synthesized from double-shelled silica@SnO_2 structures with similar shapes. The shapes and sizes of the hollow SnO_2 were almost identical to those of the silica colloidal templates. In order to obtain more information on hollow SnO_2 with different shapes, the morphology and structure of hollow SnO_2 with different shapes were investigated by FESEM, TEM and XRD.

As shown in Fig. 2a, when peanut-shaped silica colloids are used as templates, the as-prepared sample is mainly composed of peanuts with lengths of about 2 μm (Fig. 2a). Fig. 2b shows the corresponding TEM images of the sample, which indicate that the boundary of the shell of the hollow peanuts is quite defined, and the thickness of the shell is 50–100 nm.

The use of the silica colloids as the templates allows for the shape control of the resultant SnO_2 hollow structures. For example, uniform and well-defined SnO_2 hollow capsules with length of about 2 μm and width of about 1 μm (Fig. 2c) can be obtained by replacing peanuts with capsules. The structure of the sample was further characterized by TEM. As shown in Fig. 2d, the edges and centers of the capsules show strong brightness contrast, confirming their hollow nature. Each capsule-shaped structure has a shell with the thickness of 50–100 nm (Fig. 2d).

Such a novel template process can be extended to the synthesis of pseudocube-shaped hollow SnO_2. The representative SEM

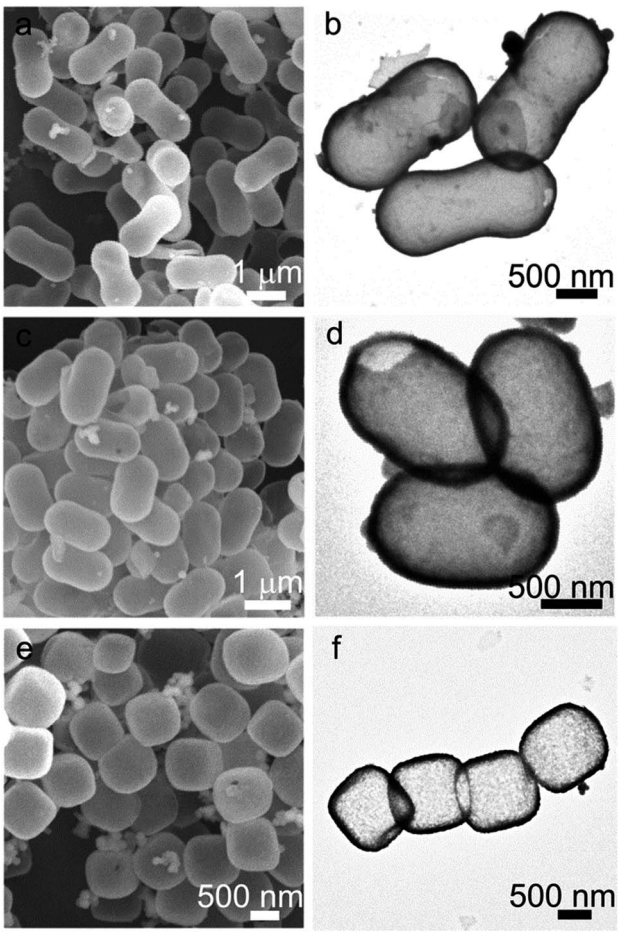

Fig. 2 FESEM and TEM images of SnO_2 hollow structures with different shapes: (a and b) peanuts; (c and d) capsules; and (e and f) pseudocubes.

patterns of the capsules shown in Fig. 2e clearly indicate that there exist a large number of pseudocubes with edge-length of about 0.8 μm. The TEM images of the final product (Fig. 2f) show that the pseudocube is empty in the interior.

The XRD patterns of the SnO_2 hollow structures with different shapes are shown in Fig. 3a–c, which exhibit somewhat broadened diffraction peaks ascribed to the tetragonal rutile phase of SnO_2 (JCPDS card no. 41-1445, space group: $P4_2/mnm$, $a_0 = 4.738$ Å, $c_0 = 3.187$ Å),[29–33] indicating that tetragonal rutile SnO_2 is the only crystalline phase existing in the obtained SnO_2 hollow structures with different shapes. The element composition is further confirmed with energy dispersive X-ray (EDX) spectroscopy analysis under TEM. EDX spectra show strong Sn and O signals (Fig. S3†). It should be noted that a trivial Si signal is detected in all spectra, which probably arises from trace amount of tin silicate formed during annealing.[23] The atomic ratio of Sn : Si for hollow peanuts, hollow capsules and hollow pseudocubes is 10.2 : 1, 10.8 : 1 and 10.8 : 1 (Fig. S3†), respectively. It indicates that the weight percent of SnO_2 in the hollow peanuts, hollow capsules and hollow pseudocubes is 96.2%, 96.4% and 96.4%, respectively.

The controlled experiment confirms that the SiO_2 templates with different shapes play an important role in the formation of

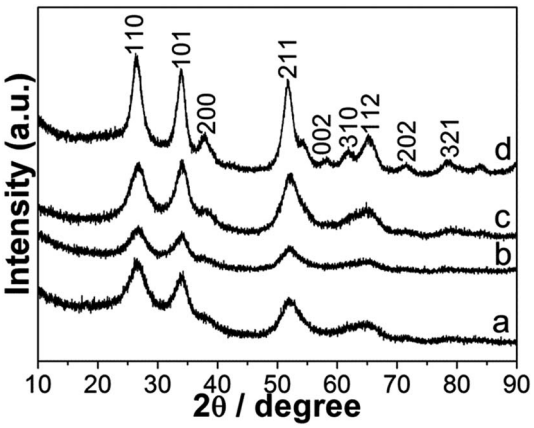

Fig. 3 XRD patterns of SnO_2 hollow structures with different shapes and solid spheres: (a) hollow peanuts, (b) hollow capsules, (c) hollow pseudocubes, (d) solid spheres.

SnO_2 hollow structures with different shapes. Without the usage of SiO_2 templates, the resultant product is composed of heavily aggregated solid spheres with diameters of 300–400 nm (Fig. 4). As shown in Fig. 3d, all of the XRD peaks observed can be assigned to the single phase SnO_2 with tetragonal rutile phase (JCPDS card no. 41-1445),[29–33] which are similar to those of SnO_2 hollow structures with different shapes (Fig. 3a–c).

The selected area electron diffraction (SAED) patterns of SnO_2 solid spheres and SnO_2 hollow structures with different shapes exhibit three sharp diffraction rings corresponding to the (110), (101), and (221) crystalline plane of the rutile-type SnO_2, confirming the formation of polycrystalline SnO_2 solid spheres and SnO_2 hollow structures with different shapes (Fig. S4†).[29–33] The high magnification TEM images reveal that SnO_2 solid spheres and SnO_2 hollow structures with different shapes are composed of tiny nanocrystallites with sizes in the range of 4–5 nm (Fig. S4c, f, i and l†). The lattice fringes of SnO_2 solid spheres and SnO_2 hollow structures with different shapes are clearly discerned and the interplanar spacing is determined to be 0.33 nm, which is in good agreement with the (110) plane of SnO_2.[29–33]

SnO_2 is a very appealing candidate as a substitute for the conventional graphite-based anode in lithium-ion batteries because of its special attributes, including high theoretical capacity (782 mA h g^{-1}), nontoxicity, improved safety, and ready availability at low cost.[23,24,29–33] In order to investigate the lithium storage performances of SnO_2 hollow structures with different shapes, SnO_2 solid spheres and different shaped SnO_2 hollow structures were used as the anode materials for lithium-ion batteries. Fig. 5a shows some representative discharge–charge curves of SnO_2 hollow structures with different shapes,

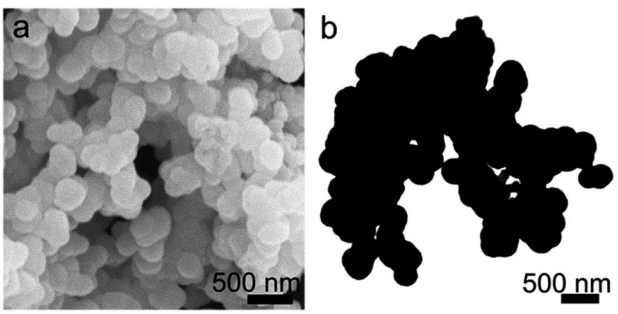

Fig. 4 (a) SEM and (b) TEM images of SnO_2 solid spheres.

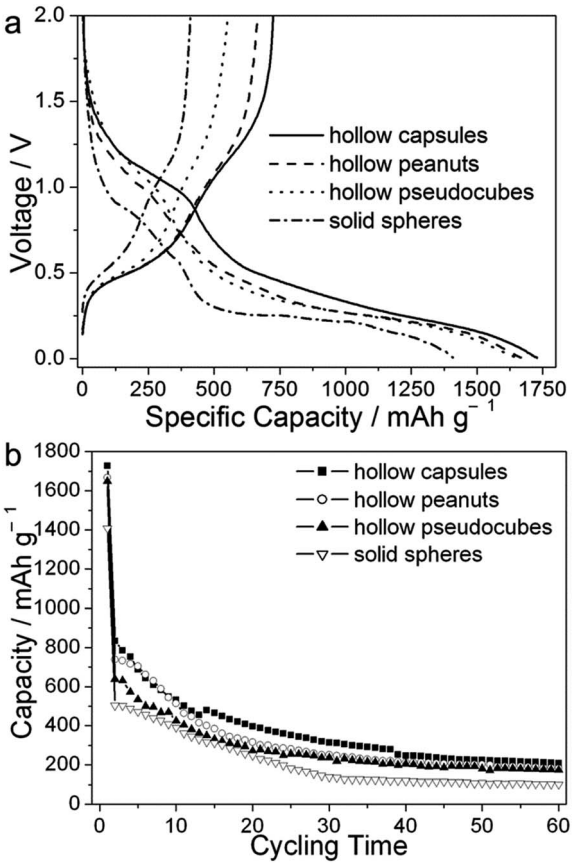

Fig. 5 (a) The first charge–discharge curves and (b) cyclic performances of SnO_2 hollow structures with different shapes and SnO_2 solid spheres tested in the potential range of 0.005–2.0 V (*vs.* Li/Li^+) at 100 mA g^{-1}.

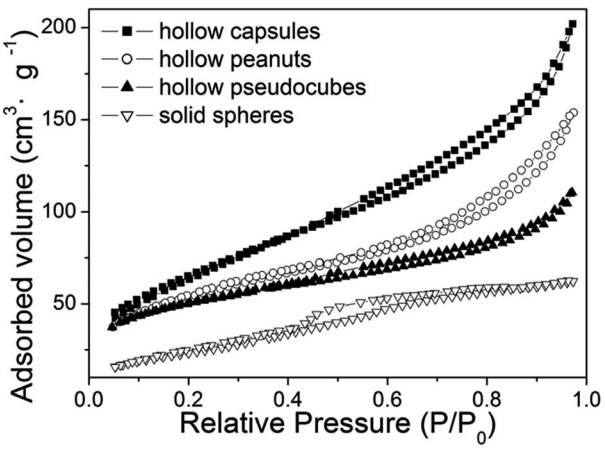

Fig. 6 The nitrogen adsorption/desorption isotherm of SnO_2 micro-scale hollow structures with different shapes and SnO_2 solid spheres.

Table 1 Electrochemical performances and specific surface areas of SnO_2 hollow particles and solid spheres

Sample	1st cycle discharge capacity/mA h g^{-1}	2nd cycle discharge capacity/mA h g^{-1}	60th cycle discharge capacity/mA h g^{-1}	Specific surface areas/m^2 g^{-1}
Hollow capsules	1728	833	208	243
Hollow peanuts	1667	740	182	192
Hollow pseudocubes	1649	639	174	171
Solid spheres	1409	504	102	89

SnO_2 solid spheres at a current density of 100 mA g^{-1} within a cutoff voltage window of 0.005–2.0 V. The obtained SnO_2 hollow capsules, hollow peanuts and hollow pseudocubes have a surprisingly large initial discharge capacity of 1728, 1667, and 1649 mA h g^{-1}, which are much higher than that of SnO_2 solid spheres, which is 1409 mA h g^{-1}. It is believed that a high surface area of SnO_2 favours efficient contact between active materials and electrolytes thereby providing more active sites for the electrochemical reactions.[30–33] As shown in Fig. 6 and Table 1, the specific surface areas of SnO_2 hollow capsules, hollow peanuts, hollow pseudocubes and SnO_2 solid spheres are 243 m^2 g^{-1}, 192 m^2 g^{-1}, 171 m^2 g^{-1} and 89 m^2 g^{-1}, respectively. The above results confirm that a decrease in specific surface area results in a decrease in the first discharge capacity. The SnO_2 hollow capsules, hollow peanuts, hollow pseudocubes and SnO_2 solid spheres are able to deliver subsequent charge capacity of 724.7, 665.4, 552.6 and 409.9 mA h g^{-1}, when charged to only 2.0 V, leading to initial irreversible losses of about 58.1%, 60.1%, 66.5% and 70.9%, respectively. The large capacity loss in the initial cycle is mainly attributed to the initial irreversible formation of Li_2O, and other irreversible processes, such as trapping of some lithium in the lattice and inevitable formation of a solid electrolyte interface (SEI) layer, which are common for most anode materials.[30–33]

Fig. 5b shows the comparative cycling performance of SnO_2 hollow capsules, hollow peanuts, hollow pseudocubes and SnO_2 solid spheres with a voltage window of 0.005–2.0 V at a current rate of 100 mA h g^{-1}. After more than 60 cycles, the high reversible capacity for SnO_2 hollow capsules, hollow peanuts and hollow pseudocubes is still found to be 208, 182 and 174 mA h g^{-1}, respectively, while the corresponding value for SnO_2 solid spheres is only 102 mA h g^{-1}, because of its much faster capacity fading. In order to further confirm the above conclusion, the coulombic efficiency has been investigated. As shown in Fig. S5,† the coulombic efficiency of these SnO_2 hollow structures and solid spheres is in the range of 29 to 42% in the first cycle, which increases to 87–94% after 5 cycles and maintains in the range of 97 to 100% for the rest cycles.

In general, the lithium storage capability of SnO_2 should be closely related to its synthesis conditions, morphology, surface area, crystalline, and so on.[23,24,29–33] It is evident that the SnO_2 hollow structures with different shapes exhibit improved lithium storage properties compared to SnO_2 solid spheres, with higher storage capability and enhanced cyclic capacity retention. It should be noted that the procedure for the synthesis of SnO_2 hollow particles with different shapes was similar to the preparation of SnO_2 solid spheres, except that different shaped SiO_2 templates were used. Therefore, we could deduce that the possible reason for the SnO_2 hollow structures with different shapes to have improved lithium storage performance is the presence of large hollow interior voids in particles with different shapes. It appears that the formation of hollow structures is beneficial to the improved lithium storage capability of SnO_2 hollow materials due to the substantial advantages of the large electrode/electrolyte interface, shortened charge/Li^+ diffusion length, and enhanced structural stability.[29–33] Examination of the electrode (without any removing of carbon black or PVDF) after 60 cycles indicates that most of the SnO_2 hollow structures with different shapes have expanded and some of them have collapsed with noticeable SnO_2 fragments (white arrows of Fig. S6†), and there have been still unbroken particles retained (black arrows of Fig. S6†).

Conclusions

In summary, uniform SnO_2 shells have been successfully deposited onto the surface of silica colloidal templates with different shapes to form double-shelled silica@SnO_2 hollow structures. After the silica is etched by HF solution, the SnO_2 hollow structures with different shapes, uniform sizes and shells are obtained. Compared with the reported procedures for hollow particles with different shapes,[23,34–37] the present approach has three main characteristics: (1) three different shapes of SnO_2 nonspherical hollow structures can be easily tailored by simply adjusting the shapes of silica colloidal templates; (2) no protective surfactant is used, so the as-prepared SnO_2 hollow structures should have relatively clean surfaces, which are important in some application areas needing strict surface chemistry requirements, such as catalysis, electrochemistry, sensing, *etc.*;[23,30,38] (3) the as-obtained SnO_2 hollow structures with different shapes have uniform sizes and shapes. The controlled experiment confirms that the silica colloidal templates with different shapes play an important role in the formation of SnO_2 hollow structures with similar shapes. Without the usage of silica colloidal templates, the resultant products are composed of solid spheres. The SnO_2 hollow structures with different shapes exhibit improved lithium storage properties compared to SnO_2 solid spheres, with higher storage capability and enhanced cyclic capacity retention. It indicates that the formation of hollow structures and high surface areas of samples are beneficial to the improved lithium storage capability of SnO_2 hollow structures

with different shapes. The above-mentioned investigations bring new insights into the influence of the structure of metal oxides on their electrochemical properties.

Acknowledgements

This work was supported by Beijing Natural Science Foundation (no. 2152010) and the General Program of Science and Technology Development Project of Beijing Municipal Education Commission (no. KM201210028019).

Notes and references

1 L. Cao, D. H. Chen and R. A. Caruso, *Angew. Chem., Int. Ed.*, 2013, **52**, 10986–10991.
2 F. Bötger-Hiller, P. Kempe, G. Cox, A. Panchenko, N. Janssen, A. Petzold, T. Thurn-Albrecht, L. Borchardt, M. Rose, S. Kaskel, C. Georgi, H. Lang and S. Spange, *Angew. Chem., Int. Ed.*, 2013, **52**, 6088–6091.
3 K. Miszta, R. Brescia, M. Prato, G. Bertoni, S. Marras, Y. Xie, S. Ghosh, M. R. Kim and L. Manna, *J. Am. Chem. Soc.*, 2014, **136**, 9061–9069.
4 C. Li, B. Jiang, M. Imura, V. Malgras and Y. Yamauchi, *Chem. Commun.*, 2014, **50**, 15337–15340.
5 S. Ching, D. A. Kriz, K. M. Luthy, E. C. Njagi and S. L. Suib, *Chem. Commun.*, 2011, **47**, 8286–8288.
6 W. J. Cai, W. Q. Wang, Y. Q. Yang, G. H. Ren and T. Chen, *RSC Adv.*, 2014, **4**, 2295–2299.
7 H. G. Wang, D. L. Ma, Y. Huang and X. B. Zhang, *Chem.–Eur. J.*, 2012, **18**, 8987–8993.
8 C. W. Sun, S. Rajasekhara, J. B. Goodenough and F. Zhou, *J. Am. Chem. Soc.*, 2011, **133**, 2132–2135.
9 C. W. Sun, J. Sun, G. L. Xiao, H. R. Zhang, X. P. Qiu, H. Li and L. Q. Chen, *J. Phys. Chem. B*, 2006, **110**, 13445–13452.
10 G. Chen, W. Ma, X. H. Liu, S. Q. Liang, G. Z. Qiu and R. Z. Ma, *RSC Adv.*, 2013, **3**, 3544–3547.
11 L. T. Lu, L. D. Tung, J. Long, D. G. Fernig and N. T. K. Thanh, *J. Mater. Chem.*, 2009, **19**, 6023–6028.
12 V. Kozlovskaya, W. Higgins, J. Chen and E. Kharlampieva, *Chem. Commun.*, 2011, **47**, 8352–8354.
13 N. C. Strandwitz, S. Shaner and G. D. Stucky, *J. Mater. Chem.*, 2011, **21**, 10672–10675.
14 N. Kang, J. H. Park, M. S. Jin, N. Park, S. M. Lee, H. J. Kim, J. M. Kim and S. U. So, *J. Am. Chem. Soc.*, 2013, **135**, 19115–19118.
15 H. B. Lin, H. B. Rong, W. Z. Huang, Y. H. Liao, L. D. Xing, M. Q. Xu, X. P. Li and W. S. Li, *J. Mater. Chem. A*, 2014, **2**, 14189–14194.
16 L. Zhou, D. Y. Zhao and X. W. Lou, *Angew. Chem., Int. Ed.*, 2012, **51**, 239–241.
17 Z. Y. Wang, D. Y. Luan, F. Y. C. Boey and X. W. Lou, *J. Am. Chem. Soc.*, 2011, **133**, 4738–4741.
18 Q. J. Yu, W. Q. Wang, H. X. Wang, Y. W. Huang, J. Z. Wang, S. Y. Gao, F. Y. Guo, X. T. Zhang, H. Gao, X. Z. Wang and C. L. Yu, *RSC Adv.*, 2015, **5**, 2586–2591.
19 X. F. Yang, J. X. Fu, C. J. Jin, J. Chen, C. L. Liang, M. M. Wu and W. Z. Zhou, *J. Am. Chem. Soc.*, 2010, **132**, 14279–14287.
20 J. Zhang, J. Guo, H. Y. Xu and B. Q. Cao, *ACS Appl. Mater. Interfaces*, 2013, **5**, 7893–7898.
21 Z. H. Dong, H. Ren, C. M. Hessel, J. Y. Wang, R. B. Yu, Q. Jin, M. Yang, Z. D. Hu, Y. F. Chen, Z. Y. Tang, H. J. Zhao and D. Wang, *Adv. Mater.*, 2014, **26**, 905–909.
22 Y. Liu, Y. Jiao, Z. L. Zhang, F. Y. Qu, A. Umar and X. Wu, *ACS Appl. Mater. Interfaces*, 2014, **6**, 2174–2184.
23 J. F. Ye, H. J. Zhang, R. Yang, X. G. Li and L. M. Qi, *Small*, 2010, **6**, 296–306.
24 W. S. Kim, Y. Hwa, J. H. Jeun, H. J. Sohn and S. H. Hong, *J. Power Sources*, 2013, **225**, 108–112.
25 X. W. Lou, C. L. Yuan and L. A. Archer, *Adv. Mater.*, 2007, **19**, 3328–3332.
26 Y. Wang, X. W. Su and S. Lu, *J. Mater. Chem.*, 2012, **22**, 1969–1976.
27 Y. Wang, X. W. Su, P. S. Ding, S. Lu and H. P. Yu, *Langmuir*, 2013, **29**, 11575–11581.
28 T. Sugimoto, M. M. Khan, A. Muramatsu and H. Itoh, *Colloids Surf., A*, 1993, **79**, 233–247.
29 S. J. Ding and X. W. Lou, *Nanoscale*, 2011, **3**, 3586–3588.
30 H. K. Wang, F. Fu, F. H. Zhang, H. E. Wang, S. V. Kershaw, J. Q. Xu, S. G. Sun and A. L. Rogach, *J. Mater. Chem.*, 2012, **22**, 2140–2148.
31 Y. L. Ding, Y. R. Wen, P. A. van Aken, J. Maier and Y. Yu, *Nanoscale*, 2014, **6**, 11411–11418.
32 X. M. Yin, C. C. Li, M. Zhang, Q. Y. Hao, S. Liu, L. B. Chen and T. H. Wang, *J. Phys. Chem. C*, 2010, **114**, 8084–8088.
33 A. Bhaskar, M. Deepa and T. N. Rao, *Nanoscale*, 2014, **6**, 10762–10771.
34 H. M. Fan, G. J. You, Y. Li, Z. Zheng, H. R. Tan, Z. X. Shen, S. H. Tang and Y. P. Feng, *J. Phys. Chem. C*, 2009, **113**, 9928–9935.
35 J. Chen, X. Wu, X. D. Hou, X. G. Su, Q. L. Chu, N. Fahruddin and J. X. J. Zhao, *ACS Appl. Mater. Interfaces*, 2014, **6**, 21921–21930.
36 D. Chen and J. H. Ye, *Adv. Funct. Mater.*, 2008, **18**, 1922–1928.
37 Y. H. Deng, H. Tüysüz, J. Henzie and P. D. Yang, *Small*, 2011, **7**, 2037–2040.
38 Q. Y. Yu, P. P. Wang, S. Hu, J. F. Hui, J. Zhuang and X. Wang, *Langmuir*, 2011, **27**, 7185–7191.

